doi:10.1016/j.jmb.2005.11.095 J. Mol. Biol. (2006) 356, 1222–1236

JMB

Available online at www.sciencedirect.com

SCIENCE DIRECT®

ELSEVIER

Structural Basis for the Requirement of Two Phosphotyrosine Residues in Signaling Mediated by Syk Tyrosine Kinase

Teresa D. Groesch†, Fei Zhou†, Sampo Mattila Robert L. Geahlen and Carol Beth Post*

Department of Medicinal Chemistry and Molecular Pharmacology, Purdue Cancer Center and Markey Center for Structural Biology, Purdue University, West Lafayette IN 47907, USA

**Corresponding author*

The protein-tyrosine kinase Syk couples immune recognition receptors to multiple signal transduction pathways, including the mobilization of calcium and the activation of NFAT. The ability of Syk to regulate signaling is influenced by its phosphorylation on tyrosine residues within the linker B region. The phosphorylation of both Y342 and Y346 is necessary for optimal signaling from the B cell receptor for antigen. The SH2 domains of multiple signaling proteins share the ability to bind this doubly phosphorylated site. The NMR structure of the C-terminal SH2 domain of PLCγ (PLCC) bound to a doubly phosphorylated Syk peptide reveals a novel mode of phosphotyrosine recognition. PLCC undergoes extensive conformational changes upon binding to form a second phosphotyrosine-binding pocket in which pY346 is largely desolvated and stabilized through electrostatic interactions. The formation of the second binding pocket is distinct from other modes of phosphotyrosine recognition in SH2–protein association. The dependence of signaling on simultaneous phosphorylation of these two tyrosine residues offers a new mechanism to fine-tune the cellular response to external stimulation.

Keywords: phosphotyrosine recognition; immune signaling; protein NMR; isotope-filter NOESY; induced-fit binding

Introduction

The engagement of immune-recognition receptors on hematopoietic cells activates multiple intracellular signaling pathways in a manner dependent on the recruitment of a Syk-family kinase to the ligated receptor. In lymphocytes, recruitment to the antigen receptor in B cells and T cells activates the protein-tyrosine kinases, Syk and ZAP-70, respectively, leading to their phosphorylation on multiple tyrosine residues.[1–5] Three of these sites are located within linker B, the region that separates the tandem SH2 domains of the kinases from their catalytic domains. In murine Syk, these are Y317, Y342, and Y346. In ZAP-70, the analogous sites are Y292, Y315 and Y319. Y317 in Syk and Y292 in ZAP-70, when phosphorylated, serve as inhibitory sites due to their interactions with members of the Cbl family of adaptor proteins, which are negative regulators of Syk family kinases.[6–8]

Y342 and Y346 in Syk, and Y315 and Y319 in ZAP-70, contribute in a positive manner to signaling such that the phosphorylation of these residues enhances the ability of each kinase to couple antigen receptors to downstream signaling pathways. The elimination of each individual tyrosine has both redundant and unique effects on signaling and the presence of both tyrosine residues is clearly required for optimal activity.[9–12] Many studies have identified effector proteins with SH2 domains that bind within this region. For example, PLCγ-1 binds to a CD8-Syk fusion protein *via* Y342 and/or Y346.[13] The elimination of both inhibits the coupling of Syk to the activation of PLCγ-2 and mobilization of Ca^{2+} in B cells.[12] Binding of the guanine nucleotide-exchange factor, Vav1, requires Syk Y342 or Zap-70 Y315 and elimination of this site inhibits signaling in mast cells

† T.D.G. & F.Z. contributed equally to this work.

Abbreviations used: PLCC, C-terminal SH2 domain of PLCγ; PDGF, platelet-derived growth factor; BCR, B cell receptor; GST, glutathione-*S*-transferase; NOE, nuclear Overhauser effect; CSP, chemical shift perturbation; HSQC, heteronuclear single quantum coherence.

E-mail address of the corresponding author: cbp@purdue.edu

and in reconstituted Syk-deficient B cells.[14–16] Finally, the replacement of Y319 in ZAP-70 inhibits the binding of both Lck and PLCγ-1 and blocks calcium mobilization in T cells.[17,18] Recent studies on the regulation of Zap-70 suggest an alternative role for these tyrosine residues analogous to that proposed for Tyr604 and Tyr610 of the EphB2 receptor.[19,20] The phosphorylation of EphB2 Tyr604 and Tyr610 creates docking sites for proteins with SH2 domains, and relieves an inhibitory interaction between the juxtamembrane region of the receptor, containing these two tyrosine residues, and the catalytic domain. For Zap-70, the substitution of Tyr315 and Tyr319 with residues other than Phe, or their complete elimination, enhances Zap-70-dependent signaling.[19]

In this study, we show that Syk Y342 and Y346 play primarily a positive rather than a negative role in coupling the antigen receptor to the activation of NFAT in B cells, and that both residues are required for optimal signaling. In examining the mechanisms by which the dual phosphorylation of this region enhances signaling, we made the interesting observation that SH2 domains from several proteins actually recognize with high affinity a single site on Syk that contains phosphotyrosine residues at both positions 342 and 346. This result is in contrast to the common SH2 recognition of a sequence with a single phosphotyrosine residue. SH2 domains that share a common fold of approximately 100 residues form a central β-sheet with two flanking α-helices. Typically SH2 domains bind a single pTyr residue in a positively charged binding pocket on one side of the central β-sheet with binding driven mainly by the interaction between the pTyr and a conserved arginine residue from the SH2 domain. While the pTyr–pocket interaction contributes most of the binding energy,[21] SH2 domains confer specificity by contacts that take place between side-chains C-terminal to the pTyr. The determination of the optimal binding sequence of many SH2 domains from studies on peptide libraries[22] led to the classification of SH2 domains into four groups determined by a single residue on the peptide-binding edge of the central β-sheet (residue βD5), which correlated with the binding specificity of the SH2 domains for the residues C-terminal to phosphotyrosine. A few exceptions to these rules have been identified but, on the whole, most of the SH2 domain interactions previously detected have followed this classification.[23] Both Y342 and Y346 of Syk individually are predicted to bind with high affinity to group I (e.g. Lck) and group II (e.g. Vav) SH2 domains, while the PLCγ C-terminal SH2 domain, a group III domain, is not predicted to bind either sequence with high affinity. However, we found that all three of these SH2 domains can bind with high affinity to this site when it is phosphorylated on both Y342 and Y346.

To establish the structural basis for SH2 recognition of a doubly phosphorylated ligand, we determined the NMR structure of the complex between the C-terminal SH2 domain of PLCγ (PLCC) and a doubly phosphorylated peptide derived from the Syk linker B region surrounding Y342 and Y346. A comparison of this structure with the previously solved structure of PLCC bound to a singly phosphorylated peptide from the platelet-derived growth factor (PDGF) receptor[24] reveals that PLCC undergoes large conformational changes upon binding the doubly phosphorylated peptide. Interestingly, these changes in conformation create a second phosphotyrosine-binding pocket to accommodate pY346 of Syk and provide electrostatic stabilization of the phosphoryl group. The formation of the secondary binding pocket is distinct from previously described modes of phosphotyrosine recognition. Residues important for the formation of the second pTyr binding pocket are conserved within the SH2 domains of proteins that share the ability to bind the doubly phosphorylated site on Syk linker B, but are missing from many other SH2 domains, suggesting that the stoichiometry of phosphorylation within this region may be used to modulate the nature of Syk–protein interactions.

Results and Discussion

Importance of Syk Y342 and Y346 for signaling

In B cells, Syk couples the B cell receptor (BCR) to the mobilization of calcium and the activation of the transcription factor, NFAT. To examine the contributions of the linker B tyrosine residues to Syk's ability to activate NFAT, we transfected Syk-deficient DT40 B cells with plasmids directing the expression of Syk or one of several Syk mutants along with a luciferase reporter plasmid driven by NFAT. The level of luciferase activity induced following receptor cross-linking is shown in Figure 1. The substitution of Y317 for phenylalanine enhanced the ability of wild-type Syk to signal. This was expected, as the role of Y317 as an inhibitory site of phosphorylation has been reported.[12] In the EphB2 receptor, the juxtamembrane region, which includes Y604 and Y610, makes extensive contacts with the N-terminal lobe of the catalytic domain to inhibit its activity.[20] A similar mechanism has been proposed for the regions of Zap-70 and Syk that surround Y315 and Y319 or Y342 and Y346, respectively.[19] To determine if the region encompassing Y342 and Y346 in Syk was inhibitory to the BCR-stimulated activation of NFAT, we deleted 20 amino acid residues from this area to generate Syk(Δ335–354) (SykΔ) and expressed this mutant in Syk-deficient DT40 cells. SykΔ exhibited a considerably reduced ability to couple the BCR to the activation of NFAT as compared to wild-type Syk (Figure 1(a)) even though it was expressed at comparable levels (Figure 1(b)). Thus, for the activation of NFAT in B cells, the major role for this region of linker B is to support rather than suppress signaling.

The contributions of Y342 and Y346 to signaling in B cells are most readily visualized in the context

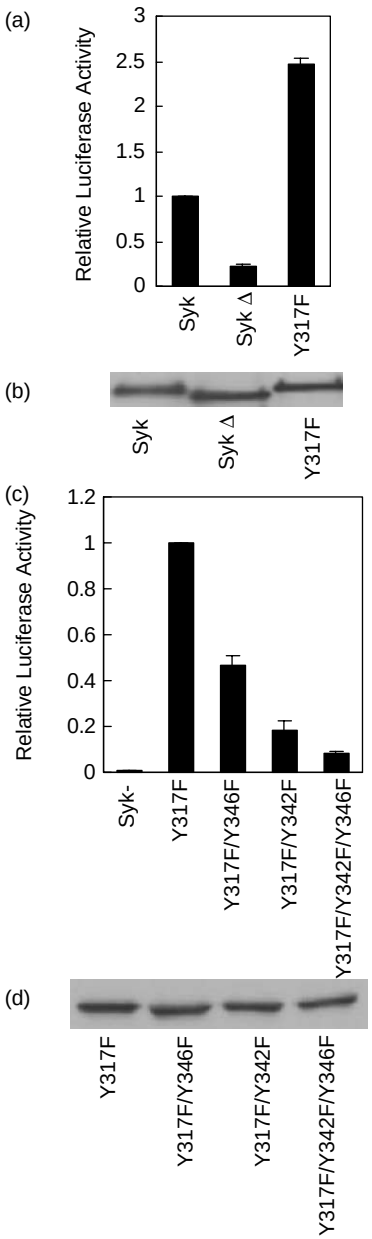

Figure 1. Effect of the replacement or elimination of linker region tyrosine residues on the Syk-dependent activation of NFAT. (a) NFAT activity in anti-IgM-treated, Syk-deficient DT40 cells transiently transfected with an NFAT-driven luciferase reporter construct and a plasmid coding for wild-type murine Syk (Syk), Syk with Y317 replaced with phenylalanine (Y317F) or Syk with residues 335–354 deleted from linker B (SykΔ). The values are compared to those obtained from cells transfected with Syk, which is normalized to a value of 1.0. (b) The relative levels of Syk expressed in the transfected cells from one trial shown in (a). (c) NFAT activity in anti-IgM-treated, Syk-deficient DT40 cells transiently transfected with an NFAT-driven luciferase reporter construct and an empty vector (Syk^-) or a plasmid encoding the indicated Syk mutant. Values were normalized to those of cells transfected with Syk(Y317F). (d) The relative levels of Syk expressed in transfected cells from one representative experiment shown in (c).

of the Syk(Y317F) mutation, which eliminates the negative regulatory site and enhances Syk's ability to couple the BCR to the mobilization of Ca^{2+} and activation of NFAT. These responses are attenuated by the removal of both Y342 and Y346.[12] However, the contributions of each individual tyrosine have not been measured. To examine this, we prepared constructs for the expression of Syk(Y317F), Syk(Y317F/Y342F), Syk(Y317F/Y346F) and Syk(Y317F/Y342F/Y346F) and transfected these into Syk-deficient DT40 B cells. The elimination of either Y342 or Y346 alone reduced the BCR-stimulated activation of NFAT (Figure 1(c)). The elimination of both residues further compromised signaling. This reduced signaling was not a consequence of lower levels of expressed protein, since comparable amounts of Syk could be detected in each set of transfected cells (Figure 1(d)). We conclude that Syk couples the BCR to the activation of NFAT most efficiently when both Y342 and Y346 are present. The presence of both tyrosine residues is required for optimal signaling in mast cells.[11]

Syk interactions with SH2 domains

To gain an understanding of how Y342 and Y346 combine to enhance signaling, we examined the mechanisms by which proteins reported to interact in this region are able to bind to Syk. We first examined the binding of phosphopeptides generated from a tryptic digest of *in vitro* autophosphorylated Syk to immobilized glutathione-*S*-transferase (GST)-SH2 domain fusion proteins derived from PLCγ-1 (Figure 2(a) and (b)), the first protein reported to bind to Syk in this region.[13] Phosphopeptides retained by the GST-SH2 domains were compared to the total digest. A single phosphopeptide was the predominant species that bound to fusion proteins containing either the C-terminal SH2 domain or both the C and N-terminal SH2 domains of PLCγ-1 (Figure 2(a)). This peptide, identified as EALPMDTEVpYESP-pYADPEEIRPK, contains phosphotyrosine residues at both positions 342 and 346.[3] The interaction between Syk-derived phosphopeptides and PLCγ-1 was specific for PLCC as no phosphopeptide was observed to bind to the N-terminal SH2 domain. Importantly, phosphopeptides containing only a single phosphate group on either Y342 or Y346, which migrate slightly higher on the alkaline gel than the doubly phosphorylated peptide, failed to bind to PLCC with sufficient affinity to be detected under these conditions. These results indicate that the phosphorylation of both Y342 and Y346 is important for the interaction of Syk with PLCC. This idea is further supported by binding studies on phosphopeptides derived from mutated Syk. No phosphopeptide bound to PLCC when it was generated from forms of Syk that contained a single point mutation at either Y342 or Y346 (Figure 2(b)).

Signaling in B cells is mediated mainly by the PLCγ-2 isoform,[25] whose C-terminal SH2 domain shares 65% sequence identity with and 81%

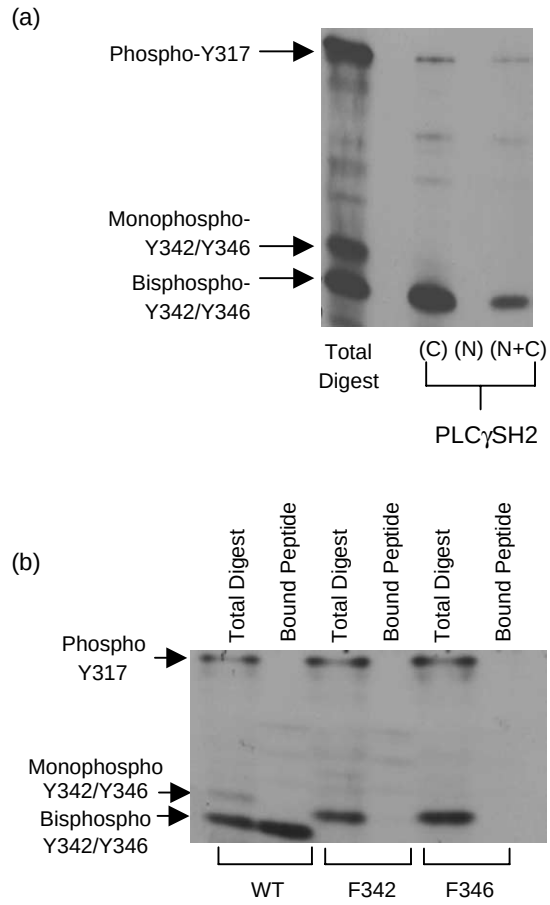

Figure 2. Binding of PLCC to phosphopeptides derived from Syk linker B. (a) The C-terminal SH2 domain of PLCγ-1 binds a Syk-derived phosphopeptide. Tryptic phosphopeptides generated from autophosphorylated Syk were applied to immobilized GST-fusion proteins that contained the C-terminal (C), N-terminal (N), or both (N+C) SH2 domains of PLCγ-1. The migration positions of the three peptides containing the linker region tyrosine residues are indicated. Y342 and Y346 lie within the same phosphopeptide, which exists in forms containing either one or two phosphotyrosine residues. (b) Phosphorylation of both Y342 and Y346 are required for high-affinity binding. Tryptic phosphopeptides were generated from *in vitro* autophosphorylated Syk, Syk(Y342F), or Syk(Y346F) and adsorbed to the immobilized GST-C-terminal SH2 domain of PLCγ-1. Bound phosphopeptides were separated by alkaline PAGE and compared to the total digest.

sequence similarity to that of PLCγ-1. To determine if PLCγ-2 shares the same preference for binding a doubly phosphorylated peptide as PLCγ-1, we prepared solid supports containing immobilized peptides corresponding in sequence to Syk amino acid residues 338–353 and containing either no phosphate group, a single phosphate group at Y342, a single phosphate group at Y346 or phosphate groups at both positions. Each resin was incubated with lysates prepared from DG75 human B cells, washed extensively and then treated with buffer containing SDS to elute bound proteins. Western blotting analyses of eluted proteins with antibodies against PLCγ-2 indicated that the protein bound preferentially to the doubly phosphorylated peptide (Figure 3(a)), indicating that the interaction of PLCC is similar for both isoforms of PLCγ.

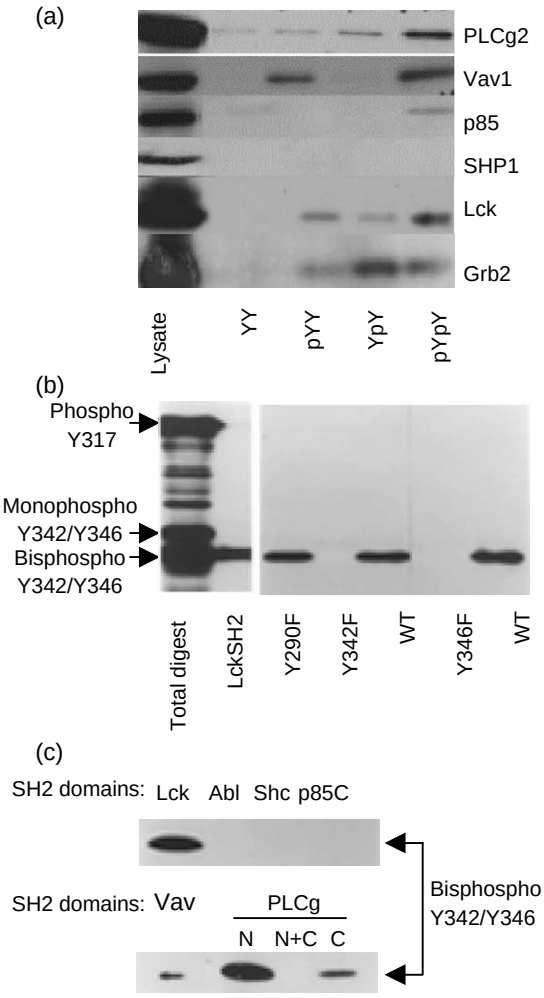

Figure 3. Binding of multiple SH2 domains to phosphopeptides derived from Syk linker B. (a) Binding of proteins to immobilized phosphopeptides. Lysates from DG75 B cells were adsorbed to resins containing immobilized peptides corresponding to residues 338–353 of Syk and containing either no phosphate group (YY), a phosphate group at Y342 (pYY), a phosphate group at Y346 (YpY) or phosphate groups at both positions (pYpY). Bound proteins were analyzed by Western blotting for the presence of PLC-γ2, Vav1, p85, SHP1 or Grb2. Lysates from Jurkat T cells were analyzed for the binding of Lck. (b) The Lck SH2 domain also binds to a doubly phosphorylated peptide. Tryptic phosphopeptides generated from autophosphorylated Syk, Syk(Y290F), Syk(Y342F) or Syk(Y346F) were adsorbed to the immobilized SH2 domain from Lck and analyzed as described in the legend to Figure 2. (c) Binding of the Syk phosphopeptide by multiple SH2 domains. Tryptic phosphopeptides generated from autophosphorylated Syk were adsorbed to immobilized SH2 domains from Lck, Abl, Shc, p85 (C-terminal domain), Vav1, or PLCγ-1. Bound peptides were eluted and analyzed as described in the legend to Figure 2.

Proteins bound to the immobilized peptide resins also were analyzed by Western blotting to detect other reported binding-partners of Syk in order to determine if any of these shared the same binding specificity. Vav1, which has been reported to require Y342 for its interactions with Syk,[14] bound to the peptide containing pY342, but not to the peptide containing pY346. Interestingly, Vav1 bound most strongly to the doubly phosphorylated peptide. This is consistent with the requirement for Y342 or both Y342 and Y346 for the robust phosphorylation of Vav1 in primary mast cells.[11] The p85 subunit of PI3K also bound selectively to the doubly phosphorylated peptide, while SHP1 did not bind to any of the peptides. Since the region surrounding Y342 and Y346 is conserved in ZAP-70, and Lck has been reported to bind in this region, we used these resins to recover proteins from lysates of Jurkat T cells. Lck bound to all three phosphopeptides, but also exhibited a preference for the doubly phosphorylated peptide. Thus, multiple SH2 domains share the ability to recognize a single site on Syk containing two phosphotyrosine residues. However, not all proteins with SH2 domains preferred binding sites with two phosphotyrosine residues. Grb2, for example, bound preferentially to the singly phosphorylated peptide containing pY346. Thus, Grb2 binds preferentially to this region when it contains one phosphotyrosine residue, but this binding is reduced when the second tyrosine residue is phosphorylated. It is interesting to note that the activation of Erk in primary mast cells is particularly sensitive to the presence of Y346.[11]

To explore further the nature of SH2 domains that bound preferentially to the doubly phosphorylated peptide, we used a total of seven GST-SH2 domain fusion proteins in phosphopeptide pull-down experiments using the assay described in Figure 2. Of these seven, three (Lck, Vav and PLCC) bound the doubly phosphorylated Y342+Y346 fragment preferentially (Figure 3(c)). In addition, the Fgr SH2 domain has been shown to select the same doubly phosphorylated peptide.[26] The remaining four SH2 domains (Shc, Abl, the N-terminal SH2 domain of PLCγ, and p85C, the C-terminal SH2 domain of the p85 regulatory subunit of phosphoinositide 3-kinase) did not bind to Syk at this site. The binding of p85 to the immobilized phosphopeptide described in Figure 3(a) is most likely a function of the N-terminal SH2 domain, as p85C binds selectively to Syk at pY317 and p85N binds elsewhere in linker B.[27]

A more complete analysis of phosphopeptide binding by the SH2 domain of Lck showed results similar to those observed for PLCC. The immobilized SH2 domain from Lck retained only the doubly phosphorylated peptide containing pY342 and pY346 (Figure 3(b)). The singly phosphorylated peptides did not bind with sufficiently high affinity to the Lck SH2 domain to be visualized in this assay where the phosphopeptides are present at very low concentrations. Furthermore, no tryptic phosphopeptides derived from either of two mutant forms of Syk containing phenylalanine substituted for Y342 or Y346 bound to the immobilized Lck SH2 domain. Substitution of an irrelevant tyrosine residue, Y290, for phenylalanine had no effect on the binding of the doubly phosphorylated peptide. These data indicate that the Lck SH2 domain, like PLCC, also binds preferentially to the doubly phosphorylated peptide. By analogy, it is likely that the phosphorylation of ZAP-70 on both Y315 and Y319 would provide a higher affinity interaction with Lck than would the phosphorylation of either site alone.

NMR structure of the Syk–PLCγ complex

To determine how a single SH2 domain could accommodate a phosphopeptide containing two phosphotyrosine residues, we solved the NMR structure of PLCC bound to DTEVpYESPpYADPE (designated pYpY) using uniformly $^{15}N/^{13}C$-labeled PLCC and unlabeled pYpY (see Experimental Procedures). PLCC was chosen for analysis, since an NMR structure of the SH2 domain bound to a singly phosphorylated peptide is available for comparative purposes.[24] Statistics for the final structures are given in Table 1.

Because of extensive chemical shift overlap in pYpY resonances, many intermolecular NOE peaks could not be assigned uniquely in the initial stage of structure calculations. A rough orientation of the peptide by initial docking with the unique intermolecular NOE assignments allowed for the assignment of additional intermolecular NOE peaks to give 29 intermolecular NOE restraints. Residues

Table 1. Structural statistics of 15 final structures

Restraints		
Protein NOE		
Intra	290	
Sequential	254	
Medium[a]	123	
Long-range[b]	204	
Ambiguous	462	
Total	1333	
Intermolecular NOE	29	
Torsion angle		
phi angles	55	
psi angles	55	
Hydrogen bond	26	
Average pairwise RMSD of ensemble	Backbone	All
Complex[c] (Å)	2.09±0.3	2.6±0.2
SH2 domain residues 10–97 (Å)	1.16±0.2	2.74±0.3
Peptide residues 1–13 (Å)	3.11±0.7	3.66±0.5
Peptide residues 3–11 (Å)	1.76±0.5	
Ramachandran plot		
Most favored region (%)	63.7	
Additionally allowed region (%)	27.5	
Generously allowed region (%)	5.9	
Disallowed region (%)	2.9	

[a] Medium-range NOEs are defined as two to three residues apart.
[b] Long-range NOEs are defined as four or more residues apart.
[c] PLCC residues 1–105 and pYpY residues 1–13.

P345 and pY346 have five and nine interactions, respectively. Residues pY342 and E350 have four NOE interactions each, residue E340 has two NOE interactions, and residues T339, E343 and P349 have a single NOE interaction. Residues D338, T339, V341, S344, A347, and D348 have no NOE interaction with the protein. While some side-chains do not contact PLCC and are without NOE interactions, the restrained regions of the peptide are spread throughout the molecule so that the overall structure is well defined.

A superposition with respect to the central β-sheet of the final 15 structures is shown in Figure 4(a). The average structure of the PLCC–pYpY complex was calculated from the 15 final structures and is shown in Figure 4(b). The pYpY peptide binds across the edge of the β-sheet in an extended conformation with residue pY342 in the primary pTyr binding pocket. The peptide backbone continues from the primary pTyr pocket along the top of the EF loop and toward the BG loop. Overall, 2028 Å^2 are buried upon pYpY binding to the SH2 domain.

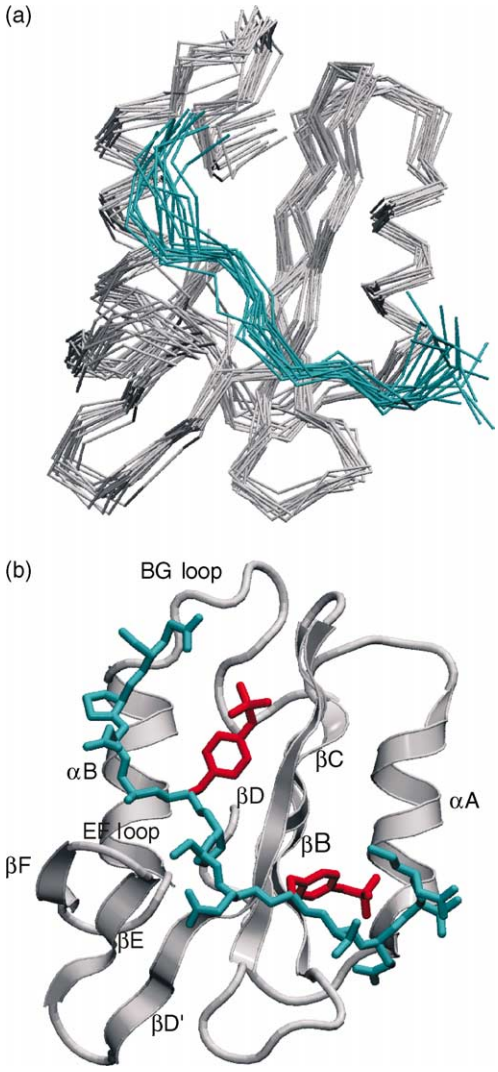

Figure 4. Structure of the PLCC-pYpY complex. (a) Overlay of the final 15 structures of the PLCC-pYpY complex (residues 10–97). The structures were aligned by the central β-sheet of PLCC. The protein is shown in grey and the peptide is shown in cyan. (b) The energy-minimized average structure of the PLCC–pYpY complex. The protein is shown in grey, and the peptide is shown in cyan with the pTyr residues highlighted in red.

The negative phosphate group of pY342 interacts with R37 of PLCC, which corresponds to the ArgβB5 residue that is conserved throughout the SH2 domain family (Figure 5(a)). The ring of the tyrosine residue also makes contacts with R39, A46, H57, and C58 (Figure 5(a)). Additional electrostatic contacts are seen between the N-terminal half of pYpY (residues E340 and E343) and PLCC (residues R18, R39, and R59), but interactions with the C-terminal half of the peptide are mainly hydrophobic in nature with the exception of pY346 (Figure 5(b)).

The interaction between PLCC and the second pTyr of the peptide (pY346) occurs on the opposite side of the central β-sheet from the primary pTyr-binding site (Figure 5(c)). A second phosphotyrosine pocket is formed, which distinguishes recognition of Syk linker B from other SH2–protein associations. Two lysine residues, K54 and K56, interact with the phosphate group and close over pY346 to form the second pTyr pocket. The pocket buries 576 Å^2 of the pTyr surface, which is more than is buried in the primary pTyr pocket (488 Å^2). The formation of the pocket results in large conformational changes in PLCC upon binding pYpY (described below).

Comparison of the pYpY-PLCC and pY1021-PLCC SH2 complexes

The structure of PLCC has been determined in complex with a singly phosphorylated peptide derived from the PDGF receptor designated pY1021 (DNDpYIIPLPDPK).[24] pY1021 has the optimal binding sequence for PLCC (pY-V/I-I/L-P) as defined by Songyang *et al.*[22] Since PLCC is classified as a group III SH2 domain, it is expected to bind peptides with a hydrophobic residue at the pTyr +1 position. In contrast, the pYpY peptide has an acidic residue following pY342, contains a large fraction of charged and polar residues, and is not predicted to bind to a group III SH2 domain. Unlike the pYpY complex, most of the side-chain interactions between pY1021 and PLCC are hydrophobic in nature, with the exception of the pTyr residue.

The peptides in the two complexes differ in their binding position as shown in Figure 6(a). The root-mean-square difference (RMSD) in the peptide C^{α} coordinates is 8.8 Å, a value significantly larger than reasonably expected from experimental uncertainty. The orientation of pYpY in the vicinity of the primary pTyr pocket is defined by intermolecular nuclear Overhauser effect (NOE) interactions of the pY342 side-chain (red, Figure 6(a)) with A46, C58, S44, and R39 of

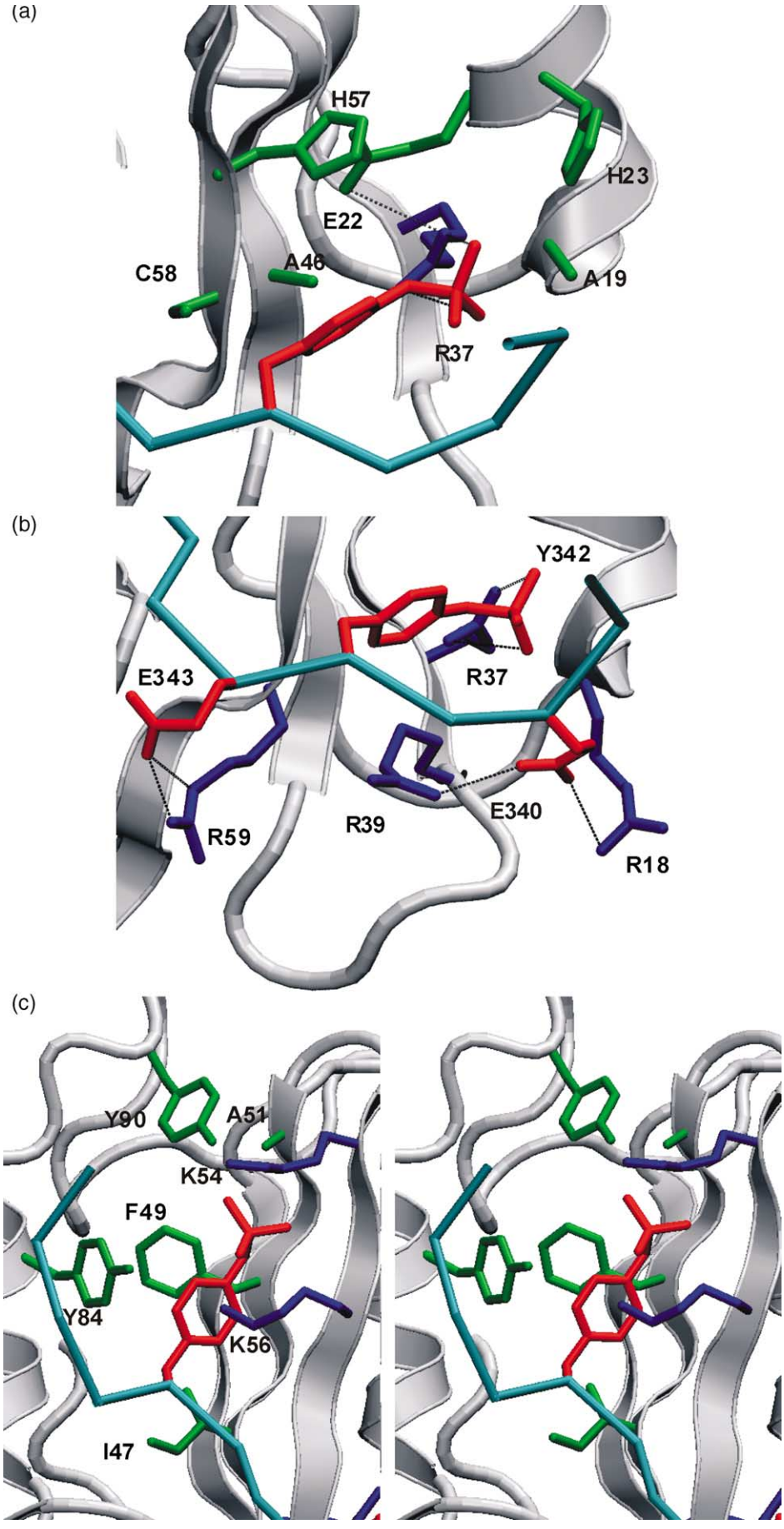
(a)
H57
H23
E22
C58
A46
A19
R37
(b)
Y342
E343
R37
R59
R39
E340
R18
(c)
Y90
A51
K54
F49
Y84
K56
I47

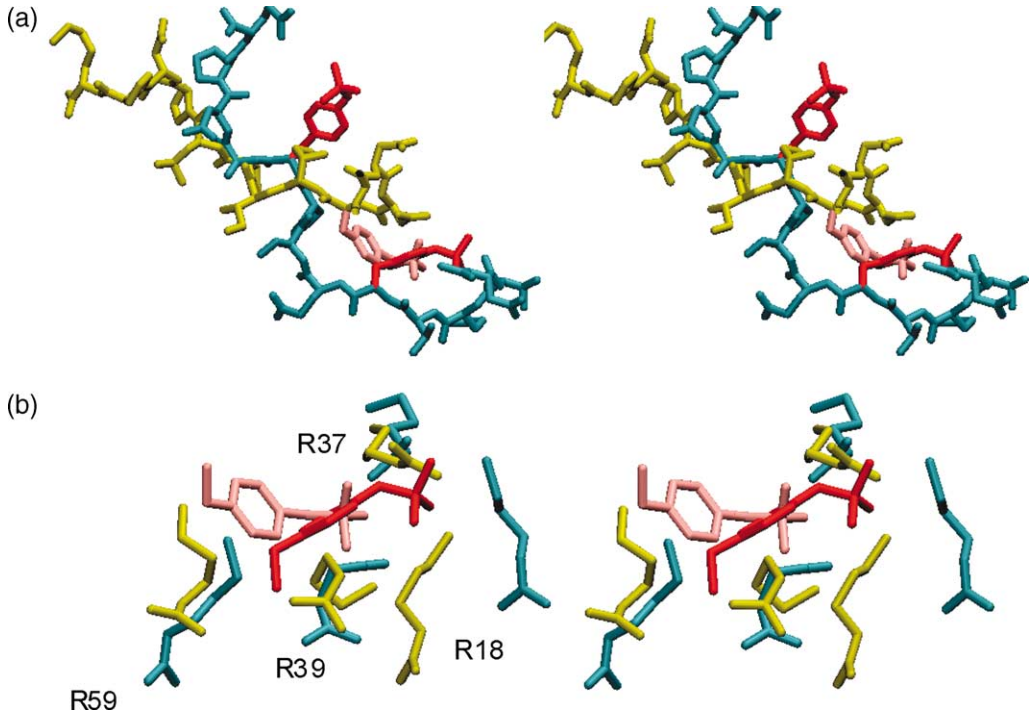

Figure 6. Comparison of the pYpY- and pY1021-PLCC complexes. (a) Stereoview of the overlay of pYpY (cyan, red) and pY1021 (yellow, pink). The structures were aligned on the basis of the central β-sheet of the proteins. The RMSD of the two peptides is 8.8 Å. (b) Stereoview of Arg residues from the primary pTyr binding site in the pYpY complex (cyan, red) and the pY1021 complex (yellow, pink).

PLCC, as well as side-chain NOE interactions of nearby residues E340 (with R39 and N40) and E342 (with E41). Together, these contacts position pY342 deeper in the pocket than the phosphotyrosine residue of pY1021, and result in the N-terminal end of helix αA being correspondingly displaced (described below). This position of the pTyr in the primary pocket affects the interactions of pTyr with the positively charged SH2 residues surrounding the pocket (Figure 6(b)). In both complexes, pTyr interacts with the conserved R37, but in the pY1021 complex, pTyr also contacts three other surrounding arginine residues: R18, R39, and R59. In the pYpY complex (cyan and red, Figure 6(b)), the position of R18 is altered by the movement of αA and consequently is too far away to interact strongly with pY342. Residues R39 and R59 are closely overlapped in the two structures but, since pTyr in the pYpY complex binds further into the pocket, the interaction with these charged residues appears less favorable. Instead of contacting pY342, these three arginine residues contribute other electrostatic interactions with pYpY (Figure 5(b)) that are not possible for pY1021 because of the hydrophobic pTyr+1 residue.

Conformational changes induced by the binding of pYpY

Figure 7(a) is an overlay of the C^{α} trace of PLCC in complex with either pYpY (grey) or pY1021 (gold) where the structures were aligned by the central β-sheet. The C^{α} RMSD between the two structures is 5.0 Å for residues 10–97. The central β-sheet of the two proteins has a C^{α} RMSD of 1.6 Å over 25 residues, and is similar, except that in the complex with pYpY there is a bulge in the βD strand such that residues K56 to C58 do not possess ideal main-chain geometry for a β-strand nor form hydrogen bonds with strand βC.

The largest difference between the pYpY and pY1021 complexes occurs in the BG loop. In the

Figure 5. (a) Interactions within the primary pTyr binding pocket. pY342 is shown in red and important residues from the protein are shown in green. Positively charged residues from the protein are shown in blue. (b) Electrostatic interactions between the N-terminal half of pYpY and PLCC. The negatively charged residues from the peptide are shown in red, and the positively charged residues are shown in blue. (c) Stereoview of interactions within the secondary binding site of the PLCC-pYpY complex. pY346 is shown in red, and important residues from the protein are shown in green. The two lysine residues that interact with pY346 (K54 and K56) are shown in blue.

structure of PLCC bound to pY1021, this loop interacts with residues from the central β-sheet and with the pTyr +1 to +3 residues of the pY1021 peptide. In the pYpY complex, the center of the BG loop moves outward by approximately 11 Å relative to its position in the pY1021 complex to expose a new surface for binding the secondary pTyr residue. Another large difference between the two structures is seen near the primary pTyr binding pocket: the orientation of αA differs in the two complexes due to the position of pY342 from pYpY in the primary pocket. There is a change in both the angle of the helix axis relative to the β-sheet as well as a 20° rotation about the helix axis. All of the large conformational differences are supported by measured NOE restraints. For example, the open

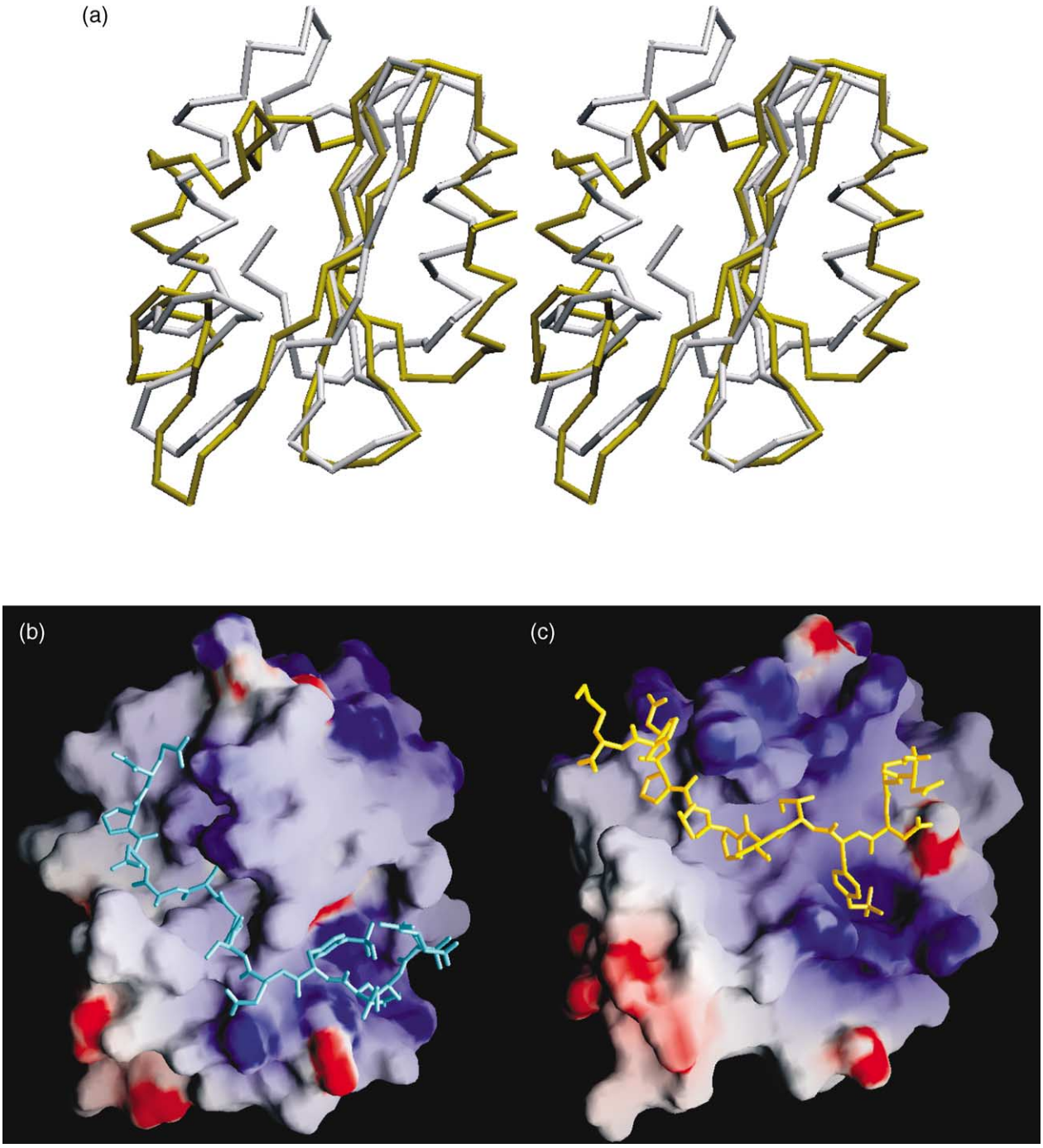

Figure 7. The binding of pYpY induces changes of conformation in PLCC. (a) Stereoview of the comparison of PLCC bound to either the singly phosphorylated pYpY (grey) or pY1021 (yellow) and aligned on the basis of the central β-sheet of the protein. Large changes exist for αA, αB, βD, the BG loop, and the secondary β-sheet. (b) Surface representation of PLCC bound to pYpY. The electrostatic potential of the proteins calculated with the program GRASP is mapped on the surface of the protein. (c) Surface representation of PLCC bound to pY1021. The two structures in (b) and (c) were aligned, and any differences between the two surfaces arise from differences in the protein conformation not protein orientation.

conformation of the BG loop is defined by NOE interactions such as Y90 (BG loop) with both A51 (βC) and E52 (CD loop), as well as interactions between K92 (BG loop) and G32 (βB). The orientation of αA is also well determined by numerous NOE interactions, including E14 and S15 with K38 (βB), L16 with R37 (βB), and M26 (αA) with S48 (βC).

Interestingly, the changes in the conformation of PLCC generate different surface topologies with distinctive electrostatic potentials. The electrostatic potential calculated with the GRASP program is mapped to the solvent-accessible surface of the pYpY complex in Figure 7(b) and the pY1021 complex in Figure 7(c). The change in the surface and electrostatic signature is obvious. Most striking is the formation of the second pTyr binding site by K54 and K56 closing over pY346 to bury the ring and hide it from view as seen in Figure 7(b). In the pY1021 complex, these two residues are highly solvated to give a more electropositive surface to the SH2 domain. Differences are evident also near the BG loop (top left in Figure 7(b) and (c)). In the pY1021 complex, the BG loop forms the upper wall of the hydrophobic binding cleft. In the pYpY complex, displacement of the BG loop exposes the hydrophobic residues (Y49, Y84, A51, I47) that were buried. The bulge in the central β-sheet of the pYpY complex is evident as well. In the pYpY complex, the bulge in βD forms a prominent ridge that increases surface contact with the pTyr+1 residue. Without the bulge, pY1021 binds along a continuous, flat surface in a hydrophobic binding cleft that extends from the pTyr pocket.

We compared the nine SH2 domains with coordinates deposited in the PDB for free and bound states or complexes with multiple ligands. The SH2 domains of Lck[28,29], Src[33], APS[30], Grb2[32], and NSyp[31] show essentially no conformational change upon peptide binding. Four of the SH2 domains (SAP/SH2D1A, p85C, and p85N) undergo relatively small conformational changes upon binding. Phosphopeptide binding to the SH2 domain of either SAP/SH2D1A[34] or p85C[35,36] causes up to a 1.3 Å displacement localized to the backbone C-terminal half of the SH2 or the secondary β-sheet, respectively. The changes are considerably smaller than those observed for PLCC. The NMR structure of p85N in the presence of a doubly phosphorylated peptide derived from the polyoma middle T antigen shows several differences relative to the unbound conformation;[37] however, it must be pointed out that alternative structures deposited in the PDB for unligated p85N SH2 domain have similarly large conformational discrepancies. Thus, the extent to which the conformational differences are the result of ligand binding is unclear.

The only previous case of an SH2 domain observed to undergo a large loop reorientation as a result of binding is Itk. The conformation change in Itk SH2 stems from isomerization of a proline residue within the CD loop that rearranges the loop and allows binding of its own SH3 domain distant from the pTyr binding pocket.[38] This conformational change is therefore not associated with protein–protein recognition of phosphotyrosine, in contrast to the induced-fit observed for PLCC.

Effect of pY346 and the second phosphotyrosine-binding pocket on PLCC–phosphopeptide interactions

Structural analyses indicate that PLCC binds pY342 in the canonical phosphotyrosine-binding site and undergoes a conformational change to accommodate pY346 in a second, previously undescribed binding pocket. To analyze the contributions of this second binding site to the phosphopeptide–SH2 domain interaction, we compared the chemical shift perturbations (CSP) in the ^{15}N-heteronuclear single quantum coherence (HSQC) spectrum of PLCC upon binding pYpY or the singly phosphorylated, Syk-derived peptide DTEVpYESPYADPE (designated pYY). CSP is the result of a change in the ^{15}N environment upon binding of a ligand from either a direct interaction with the ligand or from conformational changes within the protein. The structure of PLCC in complex with pYY could not be determined because of a lack of observable intermolecular interactions by isotope-filtered NOE spectroscopy (NOESY). The difference in the CSP between pYpY and the singly phosphorylated peptide shown in Figure 8(a) was used to determine the variations in how the two peptides bound to PLCC.

Negligible differences in CSP for residues in the primary pTyr pocket suggest that pYY binds similarly to pYpY in the N-terminal part of the peptide with pY342 in the canonical pocket. The electrostatic interactions between E340 and E343 would still be present and cause pY342 to insert further into the pocket, as seen with the pYpY structure. Larger differences were seen in the N-terminal half of βD where K54 interacts with pY346 in pYpY, as well as in the BG loop of the protein (Figure 8(b)). One large disparity is the perturbation of L89 in the BG loop. This residue is solvent-exposed in the PLCC complex with pYpY, but in the structure with pY1021, the BG loop is closed, and L89 contacts the bound peptide. The changes seen in the residues that interact with the C-terminal half of the peptide suggest that the BG loop is more like the pY1021 structure where the BG loop is closed and L89 interacts with the peptide.

To determine how the formation of this second binding pocket influences the affinity of the interaction between PLCC and the Syk-derived peptide, we assessed the binding affinities of PLCC for both pYpY and pYY. The rates and the binding constants determined from surface plasmon resonance analysis are given in Table 1. Good agreement between the kinetic rate constants and the equilibrium constants for both peptides indicates the reliability of the kinetic rates. pYpY binds to PLCC with a dissociation constant of approximately

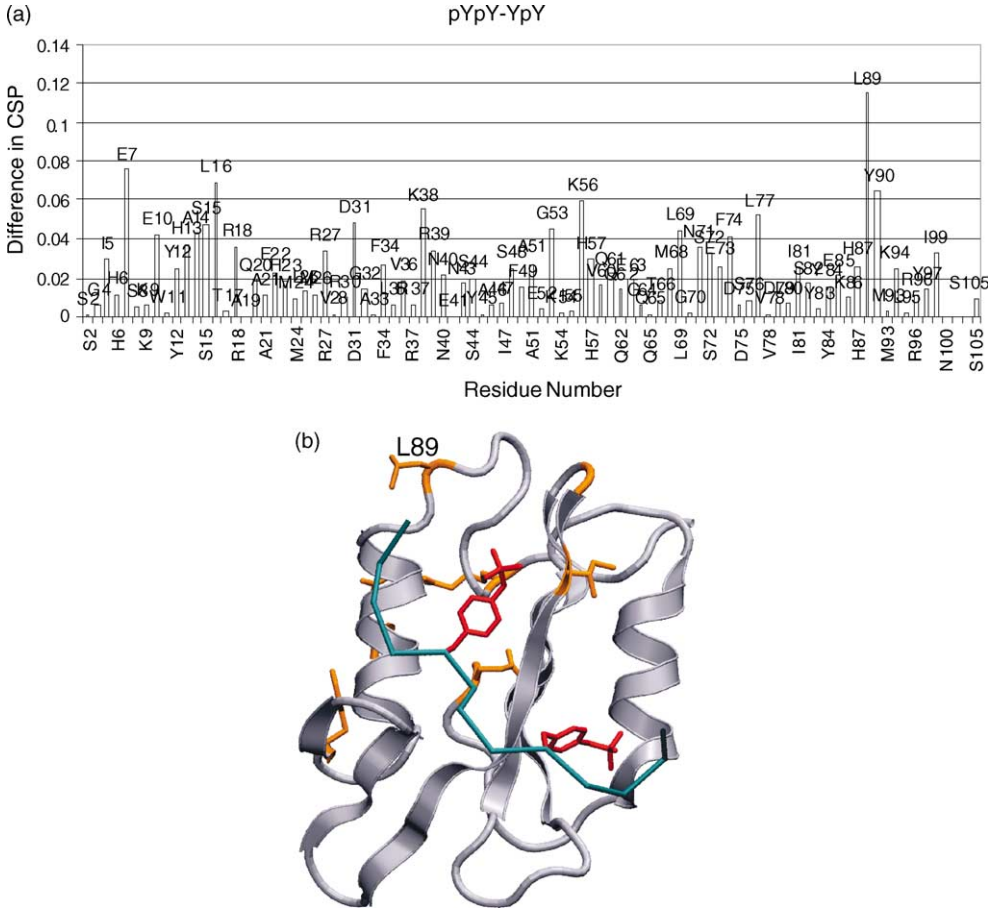

Figure 8. CSP differences between the PLCC-pYpY and -pYY complexes. (a) Differences in CSP for PLCC binding pYpY and pYY plotted as a function of PLCC residue number. (b) CSP differences between pYpY and pYY greater than 0.04 mapped onto the structure of PLCC (colored orange).

70 nM, while pYY has an approximately sevenfold decrease in the binding affinity ($K_D = 500$ nM) as a result of a slower on-rate. This decrease is apparently sufficient to prevent detection at the lower concentration levels of Figure 2(b). A change in the on-rate of an interaction may be rationalized by removal of an electrostatic interaction between the peptide and the protein. Electrostatic interactions orient the protein and its ligand, and thereby facilitate correct positioning of the ligand for binding and enhance the on-rate of the complex.

All of the SH2 domains shown to bind to the doubly phosphorylated region of Syk contain a lysine residue at position K56, while only PLCC has a second lysine residue, K54. This suggests an important interaction between K56 and pYpY. To test the contribution of K56 to the binding of pYpY, the residue was mutated to glutamine based on the corresponding residue in the N-terminal SH2 domain of PLCC that does not bind to Syk. Mutation of K56 to glutamine caused an approximate sevenfold reduction in the affinity of the PLCC for pYpY as a result of an increase in the off-rate of the interaction (Table 2), consistent with K56 contributing to the stabilization of PLCC-pYpY through electrostatic interaction with pY346. The presence of lysine at K56 likely accounts for the interactions of Lck, Fgr, Vav1 and the N-terminal

Table 2. Binding constants of PLCC measured by SPR

	PLCC-pYpY	PLCC-pYY	K56Q-pYpY
k_a ($10^6\ M^{-1}\ s^{-1}$)[a]	1.8 ($\pm$0.025)	0.27 ($\pm$0.01)	2.7 ($\pm$0.14)
k_d (s^{-1})[a]	0.12 ($\pm 2.1\times10^{-3}$)	0.13 ($\pm 1.1\times10^{-3}$)	1.2 ($\pm$0.06)
K_A ($10^6\ M^{-1}$)[b]	15.0	2.0	2.2
K_D (μM)[c]	0.066/0.070 ($\pm$0.009)	0.49/0.4 ($\pm$0.1)	0.46/0.47 ($\pm$0.13)

[a] Values for k_a and k_d are estimated from the time-dependent SPR binding curves.
[b] $K_A = k_a/k_d$.
[c] First K_D value determined from rate constants, k_a and k_d. Second K_D value estimated from the steady-state values of the SPR binding curves.

SH2 domain of p85 with the doubly phosphorylated Syk peptide. The Abl SH2 domain, the N-terminal SH2 domain of PLCγ, the Grb2 SH2 domain and the SHP1 SH2 domain all lack this residue and do not bind well to the doubly phosphorylated peptide. The one outlier we have identified so far is the C-terminal SH2 domain of p85, which has lysine in the equivalent position of K56, but does not bind the doubly phosphorylated Syk linker B, suggesting that other structural features can influence the phosphopeptide-SH2 domain interaction.

Conclusions

Following aggregation of the BCR, Syk is phosphorylated on multiple tyrosine residues, including a pair of closely spaced residues within the linker B region, Y342 and Y346. Analyses of BCR-dependent signaling in reconstituted DT40 cells indicate that phosphorylation of both residues is important for optimal signaling by a mechanism that cannot be accounted for by a release of inhibition of the catalytic domain. That Syk is phosphorylated simultaneously on both Y342 and Y346 in B cells has been documented by both metabolic labeling[3] and mass spectrometric analyses.[39] Binding studies indicate that the importance of both residues is reflected in an enhanced affinity for a subset of proteins containing SH2 domains that are able to recognize binding sites containing two phosphotyrosine residues. Examination of the structure of a doubly phosphorylated peptide bound to the C-terminal SH2 domain of PLCγ-1 indicates that each phosphotyrosine residue makes critical contributions required for a high-affinity, specific interaction.

There is considerable interest in determining how different factors influence the propagation of signals through phosphotyrosine signaling cascades. In most current models, regulation is based on the phosphorylation and interaction of one pTyr residue with a single SH2 domain. Nevertheless, there are now four structures of single SH2 domains interacting with sites containing two phosphotyrosine residues. In addition to PLCC, these include SH2 domains from p85,[37] Src[40] and the adaptor protein APS,[30] but in contrast to the PLCC complexes, none of these interactions shows substantial differences in SH2 conformation. In the case of the two phosphotyrosine residues on Syk, we find that SH2 domains from multiple binding partners (PLCγ, Vav, p85N Fgr and Lck) recognize the doubly phosphorylated site, and both phosphotyrosine residues affect signaling in cells, as well as binding affinity. Control of the relative phosphorylation of the pY342 and pY346 sites could fine-tune the response of the cell to external stimulation through the B-cell receptor by determining relative binding affinity of the specific SH2 domain-containing proteins that can interact with Syk. The B cell signaling studies demonstrate that the alternative phosphorylation states do indeed alter the amount of signal that is propagated within the cell. Syk containing only pY342 or only pY346 might signal in cells by binding to a subset of effectors that recognize each individual docking site *via* a classical SH2 domain–phosphopeptide interaction. The phosphorylation of the second tyrosine residue can then allow for further control either by enhancing the affinity of the interaction to increase the quantity of signaling or by allowing the binding of an SH2 domain with a different specificity to affect the quality of signaling. It is intriguing to also speculate that certain SH2 domains that do not contain a positively charged residue corresponding to K56 at the βD3 position can bind preferentially to the singly phosphorylated peptide over the doubly phosphorylated peptide to allow for negative regulation of SH2 binding by phosphorylation. In fact, Grb2 is a potential candidate for this type of protein. Such a mechanism could account for the differential coupling of singly phosphorylated forms of Syk to different downstream signaling pathways as has been observed in primary mast cells.[11] The solution structure of PLCC-pYpY shows that recognition of the second phosphotyrosine residue induces a substantial conformational change in the SH2 domain to form a second pTyr pocket that may be a common feature for recognition of Syk by multiple SH2 domains.

Experimental Procedures

Phosphopeptide binding assays

The preparation of tryptic phosphopeptides from *in vitro* autophosphorylated Syk and their separation by alkaline polyacrylamide gel electrophoresis have been described in detail.[3] In experiments assessing SH2 domain binding activity, proteolysis was terminated by the addition of 45 μg of soybean trypsin inhibitor. The collection of tryptic phosphopeptides was applied to 25 μl of glutathione-Sepharose containing 5 μg of immobilized GST-SH2 domain and incubated for 90 min at 4 °C. The resin was washed four times in phosphate-buffered saline containing 1% (v/v) Triton X-100 and 2 mM dithiothreitol. Bound peptides were recovered by the addition of 20 μl of alkaline PAGE sample buffer.[41] Peptides were separated by 40% alkaline-PAGE and visualized by autoradiography.[3]

The peptides DTEVYESPYADPEEIR, DTEVpYESPYADPEEIRDTEVYESPpYADPEEIR, and DTEVpYESPpYADPEEIR were purchased from SynPep. Peptides contained C-terminal amides and were covalently coupled to Affi-Gel-10 (BioRad) through the N-terminal amine. DG75 B cells or Jurkat T cells (1×10^7) were lysed in 1 ml of buffer containing 10 mM Hepes (pH 7.5), 150 mM NaCl, 5 mM EDTA, 1% (v/v) NP-40. Lysates were precleared by incubating with 12.5 μl of the resin without peptide for 1 h at 4 °C. Unbound proteins were then adsorbed to 12.5 μl of each peptide-resin at 4 °C for 2 h. Resins were washed three times with lysis buffer. Bound proteins were eluted in SDS sample buffer, separated by

SDS-PAGE, transferred to PVDF membranes and analyzed by Western blotting.

Measurement of NFAT activity

Syk-deficient chicken DT40 B cells were generously provided by Dr T. Kurosaki (Kansai Medical University, Osaka, Japan). Cells were cultured in RPMI 1640 medium supplemented with 10% (v/v) heat-inactivated fetal calf serum, 1% (v/v) chicken serum, 50 μM 2-mercaptoethanol, 1 mM sodium pyruvate, 100 IU/ml of penicillin G, and 100 μg/ml of streptomycin. cDNA for the expression of site-directed mutants was prepared using the Transformer mutagenesis kit (Clontech). Cells were transfected with 15–20 μg of Syk-expression plasmid and 10–15 μg of an NFAT-luciferase reporter construct (pNFAT Luc (Stratagene)). Cells were activated 24 h post-transfection with goat anti-chicken IgM (1–2 μg/ml) or with a combination of PMA (50 ng/ml) and ionomycin (1.0 μM) for 6 h at 37 °C. Luciferase activity was determined using the luciferase assay system kit (Promega). The values reported indicate the activity produced by anti-IgM-treatment divided by the activity produced in response to PMA + ionomycin to correct for differences in transfection efficiency and represent the average and standard error of three trials. Syk expression levels were determined by immunoblotting proteins from cell lysates with the N-19 anti-Syk antibody (Santa Cruz).

NMR sample preparation

The plasmid containing bovine PLCC (residues 663–759 from PLCγ-1) was obtained from the laboratory of Julie Forman-Kay.[24] BL21(DE3) *Escherichia coli* cells were used to express PLCC in isotopically enriched minimal medium at 20 °C. PLCC was initially purified with pTyr agarose (Sigma), and high molecular mass contaminants were removed by a Superdex-75 gel-filtration column (Amersham).

pYpY peptide was obtained in crude form from SynPep. The sequence of the peptide is DTEVpYESPpYADPE and contained an N-terminal acetyl group and a C-terminal amide. The crude peptide was purified using a Pep-RPC column (Amersham). Fractions containing eluted peptide were assessed for purity and correct sequence by matrix-assisted laser desorption/ionization (MALDI) mass spectrometry.

Final NMR samples contained 1.5 mM PLCC with a 1:1 molar ratio of protein to peptide in 20 mM Mes (pH 6.0), 100 mM NaCl and 3 mM Tris(2-carboxyethyl)-phosphine (TCEP). The stoichiometry of the complex was determined from sedimentation velocity ultracentrifugation to be 1:1. Samples used for X-filtered and 3D ^{13}C-edited [^{1}H,^{1}H] NOESY experiments were dialyzed against buffer with 90% (v/v) $^{2}H_2O$ and degassed.

NMR experiments

NMR experiments were performed either on a Varian INOVA 600 spectrometer equipped with 5 mm [^{1}H, ^{15}N, ^{13}C] triple-resonance *z*-axis pulsed-field gradient probes or a Bruker DRX 500 triple-resonance spectrometer. Sequence-specific assignments of PLCC were made using HNCACB, CBCA(CO)NH, HNCA, HCCH-TOCSY, C(CO)NH and HC(CO)NH recorded on uniformly ^{15}N/^{13}C-labeled PLCC. Aromatic resonances were assigned using 2D hbCBcgcdHD and hbCBcgcdHDHE experiments. Peptide assignments were made using 2D X-filtered intrapeptide NOESY (t_{mix} = 150 ms) and TOCSY (t_{mix} = 75 ms). Intraprotein proton–proton distance constraints were derived from 3D ^{13}C-edited [^{1}H,^{1}H] NOESY (t_{mix} = 150 ms) and 3D ^{15}N-edited [^{1}H,^{1}H] NOESY (t_{mix} = 150 ms). Intercomplex proton–proton distance constraints were derived from X-filtered NOESY (t_{mix} = 150 ms).

NMR structure calculations

Cross-peak intensity for the protein–protein NOE restraints were categorized as strong, medium, weak, and very weak, and cross-peak intensities from the X-filtered experiment were uniformly given a range between 1.8 Å and 6.0 Å. Hydrogen bond restraints were included for residues 19–28 in αA and residues 77–87 in αB. Helical ranges were identified by the ^{15}N-NOE patterns. The phi and psi angles were derived from TALOS.[42]

Structures were calculated in two stages using standard simulated annealing protocols and XPLOR-NIH.[43] The first stage involved PLCC alone with only protein–protein NMR restraints. Simulated annealing calculations of PLCC without peptide were performed using 1333 protein–protein NOE-derived restraints, 55 phi and 55 psi torsion angle restraints, and 26 H-bond restraints. The average structure was calculated from the seven best PLCC structures defined by lack of NOE violations and correct main-chain geometry. The average, energy-minimized structure of PLCC was used in the second stage of calculations to dock pYpY to the protein.

Complete assignment of the peptide resonances from intrapeptide X-filtered NOESY and TOCSY experiments was not possible because of overlapped peaks. Nonetheless, the two tyrosine residues were uniquely assigned and 16 intermolecular NOEs from these residues were used in an initial docking of the peptide to PLCC by restrained molecular dynamics. This positioning of the peptide with respect to the SH2 surface allowed assignment of all chemical shift-degenerate intermolecular NOE interactions.

In the second stage of structure calculations, the peptide was placed 12 Å from the protein and initial coordinates were in an extended strand structure. The peptide was docked to the first-stage structure of PLCC by restrained molecular dynamics using all 29 intermolecular NOE restraints. The C^{α} atoms of the protein were restrained initially, but the side-chain atoms and peptide were allowed free movement. The long-range asymptote of the NOE energy term was originally set to 0.01, and the electrostatic energy was excluded. In order to allow the peptide to move to its proper position, the van der Waals radii were reduced by a factor of 0.002. When the peptide reached a distance of approximately 5 Å from the SH2 domain, the NOE energy asymptote was increased to 1.0, and the C^{α} atoms were no longer constrained. Structures of the complex were evaluated at this point based on NOE violations, overall energy, and correct geometry. The best-scored structures were refined using simulated annealing and a force field with full van der Waals radii and electrostatics. The final structures were selected based on few NOE violations and correct geometry.

Surface plasmon resonance

All kinetic and steady state binding experiments were carried out on a BIAcore 3000 instrument (BIAcore) at 25 °C. A biotin molecule was attached to the N terminus

of pYpY and pYY by two 6-aminohexanoic acid linkers. The peptides were immobilized on SA Sensor Chips (BIAcore). Nanomolar concentrations of peptide were immobilized, and remaining streptavidin sites were blocked with free biotin. A reference flow-cell was treated by the same procedure without immobilization of the peptide.

Kinetic experiments were performed at 50 μl/min or 80 μl/min with 1 min injections of SH2 domain. Dissociation was allowed to occur for 3 min, and then the chip was regenerated with 0.05% (w/v) SDS. Kinetic constants for association, k_a, and dissociation, k_d, were calculated by BIAevaluation 3.2 software.

Steady-state experiments were performed at 15 μl/min with 1 min injections of PLCC. Dissociation and regeneration was as described above. The following equation was fit with Origin software to determine the equilibrium dissociation constant, K_D, of the complex:

$$RU = (K_D)(R_{max})/(K_D + Conc)$$

where RU is the relative response, R_{max} is the maximum response and Conc is the concentration of PLCC. Binding curves are provided as Supplementary Data.

Chemical-shift perturbations

^{15}N-labeled PLCC was prepared as described above. Purified protein was resuspended in 100 mM sodium phosphate (pH 6.5) with 3 mM DTT and 10% (v/v) ^2H_2O. Spectra were taken with increasing amounts of peptide with peptide to protein molar ratios of 0:1, 0.3:1, 0.6:1 and 1.1:1. Peaks were assigned based on the assignments for pYpY bound to PLCC.

Acknowledgements

We thank Dr John Burgner for useful discussions and assisting with BIAcore experiments. We thank Chris Isaacson for assisting with the GST pulldown experiments. This work was supported by National Institutes of Health (NIH) grants GM39478 (to C.B.P.) and CA37372 (to R.L.G.), a Purdue University reinvestment grant, and a grant to the Purdue Cancer Center (CA23568). T.D.G. was supported by a Purdue Research Foundation Fellowship and by NIH Biophysics Training Grant GM008296.

Supplementary Data

Supplementary data associated with this article can be found, in the online version, at doi:10.1016/j.jmb.2005.11.095

References

1. Hutchcroft, J. E., Harrison, M. L. & Geahlen, R. L. (1992). Association of the 72-kDa protein-tyrosine kinase Ptk72 with the B-cell antigen receptor. *J. Biol. Chem.* **267**, 8613–8619.
2. Yamada, T., Taniguchi, T., Yang, C., Yasue, S., Saito, H. & Yamamura, H. (1993). Association with B-cell-antigen receptor with protein-tyrosine kinase-P72(Syk) and activation by engagement of membrane Igm. *Eur. J. Biochem.* **213**, 455–459.
3. Keshvara, L. M., Isaacson, C. C., Yankee, T. M., Sarac, R., Harrison, M. L. & Geahlen, R. L. (1998). Syk- and Lyn-dependent phosphorylation of Syk on multiple tyrosines following B cell activation includes a site that negatively regulates signaling. *J. Immunol.* **161**, 5276–5283.
4. Chan, T. C. K., Chang, C. J., Koonchanok, N. M. & Geahlen, R. L. (1993). Selective-inhibition of the growth of Ras-transformed human bronchial epithelial-cells by emodin, a protein-tyrosine kinase inhibitor. *Biochem. Biophy. Res. Commun.* **193**, 1152–1158.
5. Neumeister, E. N., Zhu, Y. X., Richard, S., Terhorst, C., Chan, A. C. & Shaw, A. S. (1995). Binding of Zap-70 to phosphorylated T-cell receptor-Zeta and receptor-Eta enhances its autophosphorylation and generates specific binding-sites for Sh2 domain-containing proteins. *Mol. Cell. Biol.* **15**, 3171–3178.
6. Lupher, M. L., Rao, N., Lill, N. L., Andoniou, C. E., Miyake, S., Clark, E. A. *et al*. (1998). Cbl-mediated negative regulation of the Syk tyrosine kinase—a critical role for Cbl phosphotyrosine-binding domain binding to Syk phosphotyrosine 323. *J. Biol. Chem.* **273**, 35273–35281.
7. Rao, N., Lupher, M. L., Ota, S., Reedquist, K. A., Druker, B. J. & Band, H. (2000). The linker phosphorylation site Tyr(292) mediates the negative regulatory effect of Cbl on ZAP-70 in T cells. *J. Immunol.* **164**, 4616–4626.
8. Sohn, H. W., Gu, H. & Pierce, S. K. (2003). Cbl-b negatively regulates B cell antigen receptor signaling in mature B cells through ubiquitination of the tyrosine kinase Syk. *J. Expt. Med.* **197**, 1511–1524.
9. Magnan, A., Di Bartolo, V., Mura, A. M., Boyer, C., Richelme, M., Lin, Y. L. *et al*. (2001). T cell development and T cell responses in mice with mutations affecting tyrosines 292 or 315 of the ZAP-70 protein tyrosine kinase. *J. Expt. Med.* **194**, 491–505.
10. Gong, Q., Jin, X. H., Akk, A. M., Foger, N., White, M., Gong, Q. Q. *et al*. (2001). Requirement for tyrosine residues 315 and 319 within zeta chain-associated protein 70 for T cell development. *J. Expt. Med.* **194**, 507–518.
11. Simon, M., Vanes, L., Geahlen, R. L. & Tybulewicz, V. L. J. (2005). Distinct roles for the linker region tyrosines of Syk in Fc epsilon RI signaling in primary mast cells. *J. Biol. Chem.* **280**, 4510–4517.
12. Hong, J. J., Yankee, T. M., Harrison, M. L. & Geahlen, R. L. (2002). Regulation of signaling in B cells through the phosphorylation of Syk on linker region tyrosines—a mechanism for negative signaling by the Lyn tyrosine kinase. *J. Biol. Chem.* **277**, 31703–31714.
13. Law, C. L., Chandran, K. A., Sidorenko, S. P. & Clark, E. A. (1996). Phospholipase C-gamma 1 interacts with conserved phosphotyrosyl residues in the linker region of Syk and is a substrate for Syk. *Mol. Cell. Biol.* **16**, 1305–1315.
14. Deckert, M., Tartare-Deckert, S., Couture, C., Mustelin, T. & Altman, A. (1996). Functional and physical interactions of Syk family kinases with the Vav proto-oncogene product. *Immunity*, **5**, 591–604.
15. Zhang, J., Berenstein, E. & Siraganian, R. P. (2002). Phosphorylation of Tyr342 in the linker region of Syk is critical for Fc epsilon RI signaling in mast cells. *Mol. Cell. Biol.* **22**, 8144–8154.

16. Wu, J., Zhao, Q. H., Kurosaki, T. & Weiss, A. (1997). The Vav binding site (Y315) in ZAP-70 is critical for antigen receptor-mediated signal transduction. *J. Expt. Med.* **185**, 1877–1882.
17. Williams, B. L., Irvin, B. J., Sutor, S. L., Chini, C. C. S., Yacyshyn, E., Wardenburg, J. B. *et al*. (1999). Phosphorylation of Tyr319 in ZAP-70 is required for T-cell antigen receptor-dependent phospholipase C-gamma 1 and Ras activation. *EMBO J.* **18**, 1832–1844.
18. Pelosi, M., Di Bartolo, V., Mounier, V., Mege, D., Pascussi, J. M., Dufour, E. *et al*. (1999). Tyrosine 319 in the interdomain B of ZAP-70 is a binding site for the Src homology 2 domain of Lck. *J. Biol. Chem.* **274**, 14229–14237.
19. Brdicka, T., Kadlecek, T. A., Roose, J. P., Pastuszak, A. W. & Weiss, A. (2005). Intramolecular regulatory switch in ZAP-70: analogy with receptor tyrosine kinases. *Mol. Cell. Biol.* **25**, 4924–4933.
20. Wybenga-Groot, L. E., Baskin, B., Ong, S. H., Tong, J., Pawson, T. & Sicheri, F. (2001). Structural basis for autoinhibition of the EphB2 receptor tyrosine kinase by the unphosphorylated juxtamembrane region. *Cell (Cambridge, MA)*, **106**, 745–757.
21. Bradshaw, J. M., Mitaxov, V. & Waksman, G. (1999). Investigation of phosphotyrosine recognition by the SH2 domain of the Src kinase. *J. Mol. Biol.* **293**, 971–985.
22. Songyang, Z., Shoelson, S. E., Chaudhuri, M., Gish, G., Pawson, T., Haser, W. G. *et al*. (1993). Sh2 domains recognize specific phosphopeptide sequences. *Cell*, **72**, 767–778.
23. Sheinerman, F. B., Al-Lazikani, B. & Honig, B. (2003). Sequence, structure and energetic determinants of phosphopeptide selectivity of SH2 domains. *J. Mol. Biol.* **334**, 823–841.
24. Pascal, S. M., Singer, A. U., Gish, G., Yamazaki, T., Shoelson, S. E., Pawson, T. *et al*. (1994). Nuclear-magnetic-resonance structure of an Sh2 domain of phospholipase C-gamma-1 complexed with a high-affinity binding peptide. *Cell*, **77**, 461–472.
25. Carpenter, G. & Ji, Q. S. (1999). Phospholipase C-gamma as a signal-transducing element. *Expt. Cell Res.* **253**, 15–24.
26. Vines, C. M., Potter, J. W., Xu, Y., Geahlen, R. L., Costello, P. S., Tybulewicz, V. L. *et al*. (2001). Inhibition of beta 2 integrin receptor and Syk kinase signaling in monocytes by the Src family kinase Fgr. *Immunity*, **15**, 507–519.
27. Moon, K. D., Post, C. B., Dirdem, D. L., Zhou, Q., De, P., Harrison, M. L. & Geahlen, R. L. (2005). Molecular basis for a direct interaction between the Syk protein-tyrosine kinase and phosphoinositide 3-kinase. *J. Biol. Chem.* **280**, 1543–1551.
28. Eck, M. J., Atwell, S. K., Shoelson, S. E. & Harrison, S. C. (1994). Structure of the regulatory domains of the Src-family tyrosine kinase Lck. *Nature*, **368**, 764–769.
29. Eck, M. J., Shoelson, S. E. & Harrison, S. C. (1993). Recognition of a high-affinity phosphotyrosyl peptide by the Src homology-2 domain of P56(Lck). *Nature*, **362**, 87–91.
30. Hu, J. J., Liu, J., Ghirlando, R., Saltiel, A. R. & Hubbard, S. R. (2003). Structural basis for recruitment of the adaptor protein APS to the activated insulin receptor. *Mol. Cell.* **12**, 1379–1389.
31. Kay, L. E., Muhandiram, D. R., Wolf, G., Shoelson, S. E. & Forman-Kay, J. D. (1998). Correlation between binding and dynamics at SH2 domain interfaces. *Nature Struct. Biol.* **5**, 156–163.
32. Nioche, P., Liu, W. Q., Broutin, I., Charbonnier, F., Latreille, M. T., Vidal, M. *et al*. (2002). Crystal structures of the SH2 domain of Grb2: highlight on the binding of a new high-affinity inhibitor. *J. Mol. Biol.* **315**, 1167–1177.
33. Waksman, G., Kominos, D., Robertson, S. C., Pant, N., Baltimore, D., Birge, R. B. *et al*. (1993). Crystal structure of the phosphotyrosine recognition domain Sh2 of V-Src complexed with tyrosine phosphorylated peptides. *Nature*, **358**, 646–653.
34. Hwang, P. M., Li, C. J., Morra, M., Lillywhite, J., Muhandiram, D. R., Gertler, F. *et al*. (2002). A 'three-pronged' binding mechanism for the SAP/SH2D1A SH2 domain: structural basis and relevance to the XLP syndrome. *EMBO J.* **21**, 314–323.
35. Breeze, A. L., Kara, B. V., Barratt, D. G., Anderson, M., Smith, J. C., Luke, R. W. *et al*. (1996). Structure of a specific peptide complex of the carboxy-terminal SH2 domain from the p85 alpha subunit of phosphatidylinositol 3-kinase. *EMBO J.* **15**, 3579–3589.
36. Siegal, G., Davis, B., Kristensen, S. M., Sankar, A., Linacre, J., Stein, R. C. *et al*. (1998). Solution structure of the C-terminal SH2 domain of the p85 alpha regulatory subunit of phosphoinositide 3-kinase. *J.M. Biol.* **276**, 461–478.
37. Weber, T., Schaffhausen, B., Liu, Y. X. & Gunther, U. L. (2000). NMR structure of the N-SH2 of the p85 subunit of phosphoinositide 3-kinase complexed to a doubly phosphorylated peptide reveals a second phosphotyrosine binding site. *Biochemistry*, **39**, 15860–15869.
38. Mallis, R. J., Brazin, K. N., Fulton, D. B. & Andreotti, A. H. (2002). Structural characterization of a proline-driven conformational switch within the Itk SH2 domain. *Nature Struct. Biol.* **9**, 900–905.
39. Salomon, A. R., Ficarro, S. B., Brill, L. M., Brinker, A., Phung, Q. T., Ericson, C. *et al*. (2003). Profiling of tyrosine phosphorylation pathways in human cells using mass spectrometry. *Proc. Natl Acad. Sci. USA*, **100**, 443–448.
40. Lubman, O. Y. & Waksman, G. (2003). Structural and thermodynamic basis for the interaction of the Src SH2 domain with the activated form of the PDGF beta-receptor. *J. Mol. Biol.* **328**, 655–668.
41. West, M. H. P., Wu, R. S. & Bonner, W. M. (1984). Polyacrylamide-gel electrophoresis of small peptides. *Electrophoresis*, **5**, 133–138.
42. Cornilescu, G., Delaglio, F. & Bax, A. (1999). Protein backbone angle restraints from searching a database for chemical shift and sequence homology. *J. Biomol. NMR*, **13**, 289–302.
43. Schwieters, C. D., Kuszewski, J. J., Tjandra, N. & Clore, G. M. (2003). The XPLOR-NIH NMR molecular structure determination package. *J. Magn. Reson.* **160**, 66–74.

Edited by M. F. Summers

(Received 22 September 2005; received in revised form 30 November 2005; accepted 30 November 2005)
Available online 27 December 2005

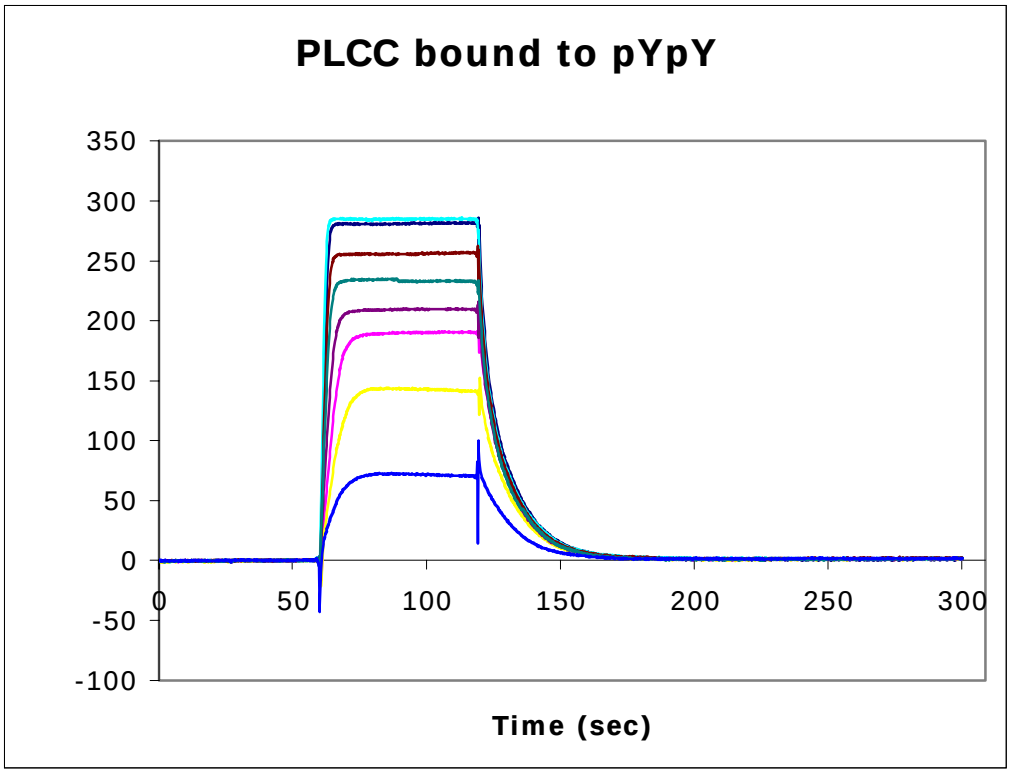

Supplement 1. Binding curves of PLCC binding to immobilized pYpY. Nanomolar concentrations of biotinylated pYpY peptide were immobilized on a streptavidin coated sensor chip. Concentrations of PLCC from 25 to 300 nM were used for determination of the kinetic rates of binding.

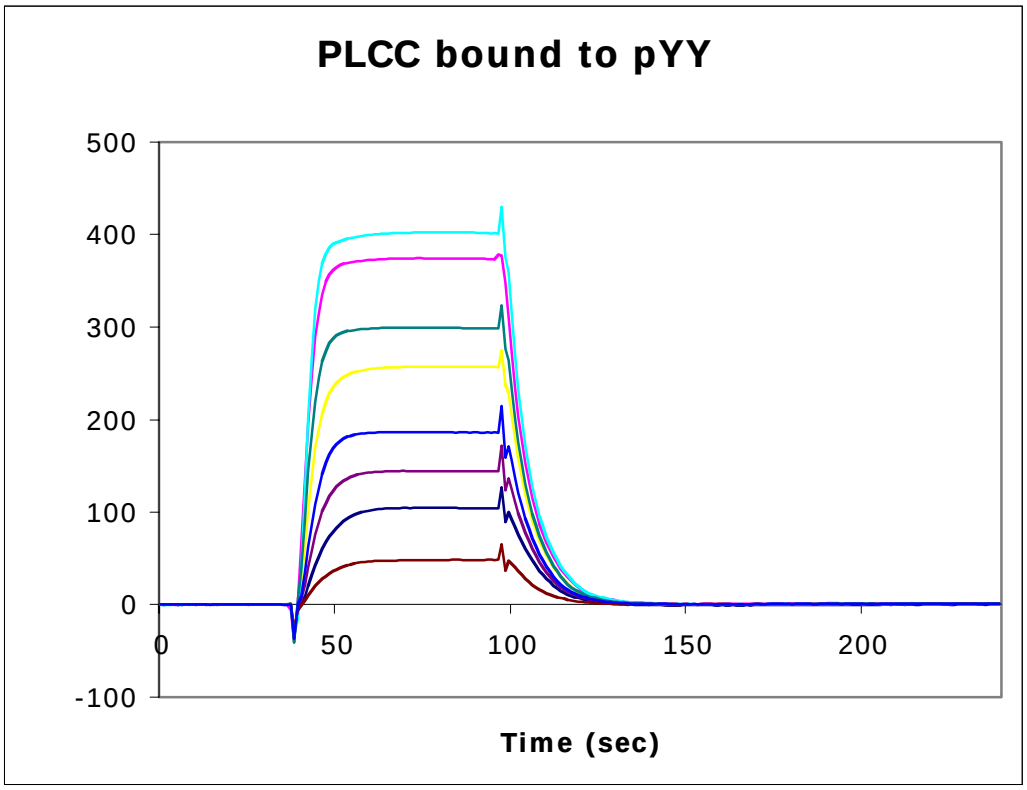

Supplement 2. Binding curves of PLCC binding to immobilized pYY. Nanomolar concentrations of biotinylated pYY peptide were immobilized on a streptavidin coated sensor chip. Concentrations of PLCC from 25 to 300 nM were used for determination of the kinetic rates of binding.